OPEN ACCESS Freely available online

PLoS GENETICS

Global Analysis of the Impact of Environmental Perturbation on *cis*-Regulation of Gene Expression

Elin Grundberg[1,2,¤*], Veronique Adoue[1,2], Tony Kwan[1,2], Bing Ge[2], Qing Ling Duan[3], Kevin C. L. Lam[2], Vonda Koka[2], Andreas Kindmark[4], Scott T. Weiss[3], Kelan Tantisira[3], Hans Mallmin[5], Benjamin A. Raby[3], Olle Nilsson[5], Tomi Pastinen[1,2,6]

1 Department of Human Genetics, McGill University, Montréal, Quebec, Canada, **2** McGill University and Genome Québec Innovation Centre, Montréal, Quebec, Canada, **3** Channing Laboratory, Department of Medicine, Brigham and Women's Hospital, Harvard Medical School, Boston, Massachusetts, United States of America, **4** Department of Medical Sciences, Uppsala University, Uppsala, Sweden, **5** Department of Surgical Sciences, Uppsala University, Uppsala, Sweden, **6** Department of Medical Genetics, McGill University, Montréal, Quebec, Canada

Abstract

Genetic variants altering *cis*-regulation of normal gene expression (*cis*-eQTLs) have been extensively mapped in human cells and tissues, but the extent by which controlled, environmental perturbation influences *cis*-eQTLs is unclear. We carried out large-scale induction experiments using primary human bone cells derived from unrelated donors of Swedish origin treated with 18 different stimuli (7 treatments and 2 controls, each assessed at 2 time points). The treatments with the largest impact on the transcriptome, verified on two independent expression arrays, included BMP-2 (t = 2h), dexamethasone (DEX) (t = 24h), and PGE_2 (t = 24h). Using these treatments and control, we performed expression profiling for 18,144 RefSeq transcripts on biological replicates of the complete study cohort of 113 individuals ($n_{total} = 782$) and combined it with genome-wide SNP-genotyping data in order to map treatment-specific *cis*-eQTLs (defined as SNPs located within the gene ±250 kb). We found that 93% of *cis*-eQTLs at 1% FDR were observed in at least one additional treatment, and in fact, on average, only 1.4% of the *cis*-eQTLs were considered as treatment-specific at high confidence. The relative invariability of *cis*-regulation following perturbation was reiterated independently by genome-wide allelic expression tests where only a small proportion of variance could be attributed to treatment. Treatment-specific *cis*-regulatory effects were, however, 2- to 6-fold more abundant among differently expressed genes upon treatment. We further followed-up and validated the DEX–specific *cis*-regulation of the *MYO6* and *TNC* loci and found top *cis*-regulatory variants located 180 kb and 250 kb upstream of the transcription start sites, respectively. Our results suggest that, as opposed to tissue-specificity of *cis*-eQTLs, the interactions between cellular environment and *cis*-variants are relatively rare (~1.5%), but that detection of such specific interactions can be achieved by a combination of functional genomic approaches as described here.

Citation: Grundberg E, Adoue V, Kwan T, Ge B, Duan QL, et al. (2011) Global Analysis of the Impact of Environmental Perturbation on *cis*-Regulation of Gene Expression. PLoS Genet 7(1): e1001279. doi:10.1371/journal.pgen.1001279

Editor: Greg Gibson, Georgia Institute of Technology, United States of America

Received September 6, 2010; **Accepted** December 17, 2010; **Published** January 20, 2011

Funding: This work was supported by Genome Quebec, Genome Canada (GC-Comp-III), and the Canadian Institutes of Health Research (CIHR). The CAMP Genetics Ancillary Study is supported by grant R01 HL086601, U01 HL075419, U01 HL65899, P01 HL083069, and T32 HL07427 from the National Heart, Lung, and Blood Institute, National Institutes of Health (NIH/NHLBI); through the Colorado CTSA grant 1 UL1 RR025780 from the NIH and National Center for Research Resources (NCRR); and from grants R01 HL086601 and RC2 HL101543. The funders had no role in study design, data collection and analysis, decision to publish, or preparation of the manuscript.

Competing Interests: The authors have declared that no competing interests exist.

* E-mail: eg5@sanger.ac.uk

¤ Current address: The Wellcome Trust Sanger Institute, Hinxton, United Kingdom

Introduction

The genetic contribution to population variation in *cis*-regulation of gene expression has been well studied in expression QTL (eQTL) studies where genome-wide expression profiles in cells or tissues of interest are statistically linked to sequence variants, known as "expression SNPs" or eSNPs. Following the pioneering of mapping eQTLs using Epstein-Barr virus transformed lymphoblastoid cell lines (LCLs) [1] such as those analyzed in the HapMap project [2,3], various primary cells [4–8] and complex tissues [5,8–10] have been used for the identification of *cis*-regulatory variants. These eQTL studies have all been able to show a strong effect of common *cis*-variants on gene expression as compared to *trans*-effects that are more difficult to detect due to smaller effect sizes [7]. More recently, eQTL studies have included multiple cell types from the same study population where results have pointed towards a substantial proportion of *cis*-effects being reproducible across different cell types [11]. However, although a large proportion of the *cis*-effects seem to be cell-type invariant, others may act in a cell-type specific manner [4,11].

Environmental factors influence gene expression, and undoubtedly interaction between sequence variants and environmental stimuli represents a critical step to cellular development and disease pathogenesis. Modeling gene-environment interactions in a clinical setting is challenging, but eQTL mapping may represent an excellent model for identifying these important interactions that impact phenotype. Smirnov et al [12] studied inter-individual differences in expression in response to radiation in LCLs and found that most regulators influencing radiation-induced gene expression act in *trans* with very few *cis*-regulatory effects.

Author Summary

Population variation in normal gene expression has been convincingly shown to be under strong genetic control where the main genetic variants are located within close proximity to the gene itself (so called *cis*-acting). However, the extent to which controlled, environmental stimuli influences *cis*-regulation of gene expression is unclear. Here, we combine different functional genomic approaches and examine the role of common genetic variants on induced gene expression in a population panel of primary human cells derived from ~100 unrelated donors treated under multiple conditions. Using these approaches, we find that the interaction between cellular environment and *cis*-variants are relatively rare, with only a small proportion of the identified genetic variants being specific to treatment. However, although treatment-specific genetic regulation of gene expression seems to be infrequent, we prove its existence by thorough validation of treatment-specific effects of the glucocorticoid-specific regulation of *TNC* expression. Taken together, these findings indicate that the regulatory landscape within a cell is very stable but, by combining functional genomic tools gene-environmental interactions of clinical importance, can be detected and possibly used as biomarkers in future pharmacogenomic studies.

Similarly, in a recent report studying the effect of pro-inflammatory oxidized phospholipids on global gene expression in human primary endothelial cell lines, the majority of the regulated transcripts were shown to be influenced by *trans*-acting loci [13].

In an attempt to elucidate the impact of non-genetic, experimental factors such as growth conditions on eQTL mapping in cultured cells, we previously studied multiple primary cell lines derived independently from the same individual, and assessed the replicability of *cis*- versus *trans*-associations using these biological replicates. We found that *cis*-eQTLs are highly reproducible across biological replicates, as compared to *trans*-eQTLs that showed much lower than expected overlap across replicates [7]. Clearly, larger sample sizes are needed in order to find SNPs with true *trans* regulatory effects on gene expression.

To explore the impact of environmental perturbation on *cis*-regulation (defined here as variants located within the gene or in a $\pm$250kb window flanking the gene) of human gene expression, we performed large-scale induction experiments using human primary osteoblasts (HOb) from a population panel described previously [7,14]. Environmental stimuli included growth factors [15,16], cytokines [17,18] and hormones [19–21], all with previous known effects on the osteoblast transcriptome. We verified that the response upon treatment was robust before proceeding with *cis*-eQTL analysis. In addition to standard eQTL mapping, we applied an alternative approach with improved sensitivity for mapping *cis*-regulatory variants based on the measurement of allele-specific expression (AE) that directly demonstrates that a variant acts in *cis* [11,22,23]. We employed the Illumina HumanOmni1-Quad BeadChip for global assessment of AE - an approach based on the quantitative assessment of allele ratios in expressed heterozygous SNPs in RNA samples, which are then normalized to corresponding genomic DNA heterozygote ratios. An outline of the study is presented in Figure 1. Using these approaches we find that the *cis*-regulatory landscape within a cell is very stable, with only a small proportion of the identified *cis*-eQTLs being specific to environmental stimuli.

Results

Differential gene expression upon environmental perturbation

Human osteoblast-like cells (HOb) derived from 113 unrelated Swedish donors, each with independently derived primary cell lines (n = 3), were cultured under 18 different conditions: seven different treatments (BMP-2, dexamethasone (DEX), IGF1, PTH, PGE_2, TNFα, 1.25VitD_3) and two controls, each at two time points (2h and 24h, respectively). To identify those conditions that most clearly influenced global gene expression, we first performed a pilot study, assessing the response of each treatment on gene expression upon treatment in three biological replicates for one individual using Affymetrix GeneChip U133+2 arrays. In general, all treatments demonstrated significantly more genes that were up- or down-regulated after 24h exposure than at the earlier time point (FDR adjusted P value$<$0.05 and Fold change $>$2) (Figure 2A and Figure S1A). Based on both magnitude and biological relevance of regulated genes, BMP-2, DEX and PGE_2 were chosen for the subsequent global analysis of the effect of environmental perturbation on *cis*-regulation. DEX and BMP-2 treatment regulate the expression of several immediate-early (2h exposure) and late (24h exposure) genes and pathways related to bone cell function as previously described [14]. For instance, upon stimulation with BMP-2 for 2h, a large number of negative regulators are up-regulated including the inhibitory Smads (*SMAD6* and *SMAD7*) and the BMP inhibitor, *Noggin*. In DEX-treated samples, the IGF1 signaling pathway is one of the top canonical signaling pathways down-regulated following stimulation. We further analyzed the genes regulated by PGE_2 and found them significantly associated with skeletal development and function including growth ($P = 3\times10^{-4}$, Fisher's exact test), differentiation ($P = 3\times10^{-4}$, Fisher's exact test) and formation of bone cells ($P = 9\times10^{-4}$, Fisher's exact test).

To verify that the observed responses upon treatment were robust across expression platforms, we profiled one additional individual using Illumina HumanRef8 v2 BeadChips and again found that stimulation by DEX, BMP-2 and PGE_2 resulted in the most striking gene expression changes (Figure 2B) with modest to weak effects of the remaining treatments (Figure S1B). The proportions of differentially expressed genes (1-pi0) among all tested genes for the three treatments are presented in Table S1. In addition, complete lists of response genes upon treatment are shown in Tables S2, S3, S4. We have previously validated response genes upon DEX and BMP-2 treatment [14] by real-time RT-PCR, and upon PGE_2 stimulation in this study, and in all cases the direction of effect was the same (Figure S2).

We then obtained whole genome expression profiles from the cultured primary cells that were untreated (t = 24h, N = 94) and treated with DEX (t = 24h, N = 107), BMP-2 (t = 2h, N = 101), PGE_2 (t = 24h, N = 100), each with at least two biological replicates, using Illumina HumanRef8 v2 arrays. For each individual, we averaged the normalized expression scores across biological replicates to obtain a single measure for each of the 18,144 genes included on the array.

We further studied whether responses upon DEX, BMP-2 and PGE_2 treatments seen in a single sample as described above using Affymetrix GeneChips accurately represented a general effect in the study population. Approximately 13,000 RefSeq transcripts overlapped the two studies and the expression response for each treatment from the different studies was used in a correlation analysis (median log2 fold change was used as an estimate of the general effect in the study population). We found strong correlations (r = 0.5–0.6) of expression changes by individual

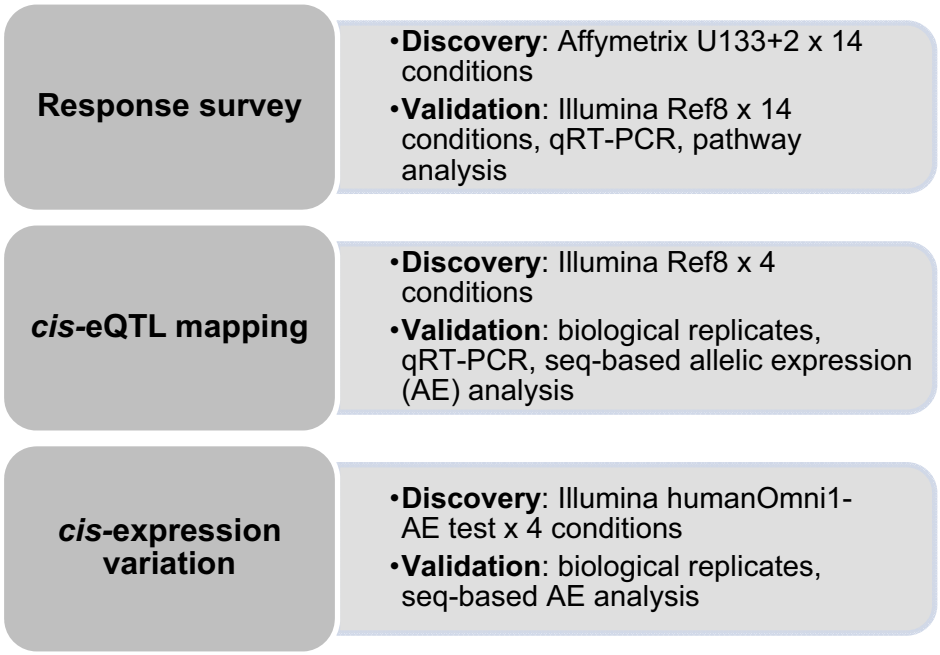

Figure 1. Study outline.
doi:10.1371/journal.pgen.1001279.g001

genes from the different studies (Figure S3) indicating that the selected treatments robustly impact the expression profiles in the study population.

Mapping of *cis*-eQTLs upon perturbation

The samples included here have previously been genotyped using the Illumina Hap550K arrays and were included in our recent work of *cis*-eQTL analysis focused on the untreated control samples from the same study population [7]. All probes overlapping a SNP (dbSNP 126) were removed as previously described resulting in ~17,000 probes included in the eQTL analyses. The conditioned expression traits were used as dependent variables in linear regression models and adjusted for sex and year of birth. Our analysis focused on *cis*-regulatory variants defined as SNPs (N = 388,946) located in a 250kb window flanking the target transcript [7].

Summary statistics from the *cis*-eQTL analyses are presented in Table 1 and in Figure S4 using all samples (n = 94–101) and in Table S5 separating the biological replicates in identical samples across treatments (n = 80). Characteristics of all significant, independent *cis*-variants (5% FDR) including distance to transcription start site (TSS) and SNP category (i.e. intronic, 3′UTR, coding etc) are presented in Table S6 and Figure S5. At all three significance levels (Bonferroni $P<3.5\times10^{-8}$, 1% FDR, and 5% FDR), we identified on average ~40% more *cis*-eQTLs in induced samples as compared to the untreated controls. However, when we compared top ranked *cis*-eQTLs between treatments we found a high overlap of significant associations across treatments (Figure 3). Despite clear global effects of each treatment to expression profiles, genes under genetic *cis*-regulatory component demonstrate very similar dependence on local variants. For example, 93% of *cis*-eQTLs identified in DEX treated samples at 1% FDR ($P<2.5\times10^{-5}$) are observed in at least one other condition at a slightly less stringent P-value threshold of $P=5\times10^{-4}$. The overlap changes only slightly when considering independent signals (87% versus 93%). This degree of overlap across treatment groups is similar to the proportion of shared *cis*-eQTLs between two biological replicates, as previously described [7]. Similarly, when we restrict analysis to significant *cis*-eQTLs (1% FDR) in DEX-treated samples, we note strong enrichments of low P-values in the eQTL analysis for both of the other treatments (BMP-2, PGE_2) and in the untreated control samples, confirming that the vast majority of observed eQTL associations are observed regardless of experimental condition (Figure S6). We then asked whether the shared *cis*-eQTLs across treatments are for genes that significantly respond to each treatment or if they are expressed, but not differentially expressed. We classified the genes as responders (significant >1.5-fold difference in expression upon induction) and non-responders based on the pilot data (Table S2, S3, S4) but found no difference in the proportion of overlapped *cis*-eQTLs between the two lists of genes.

We defined high-confidence environmental-specific *cis*-eQTLs as being 1) significant in one treatment at 1% FDR or 5% FDR, respectively, and 2) non-significant ($P>0.05$) in all three remaining conditions. As expected based on the results from the initial analysis described above, treatment-specific *cis*-eQTLs were found to be rare. At 1% FDR, we identified on average 1.4% treatment-specific *cis*-eQTLs, representing only a slight excess to the expected false discovery rate (Table 2). When restricting to independent *cis*-eQTLs only, the treatment specificity at 1% FDR was increased to ~2.5% (all treatment-specific *cis*-eQTLs at 5% FDR are presented in Table S7, S8, S9). The identified high-confidence *cis*-eQTLs at 5% FDR corresponded to 72–143 genes per treatment group (Table 2) where we found evidence of a ~2-fold enrichment of treatment-specific expression pattern for the DEX-specific genes harboring an eQTL, than expected by chance (binomial $P<0.05$). No such enrichment was seen for the BMP-2 or PGE_2 specific associations.

We further analyzed the genes harboring treatment-specific *cis*-eQTLs for enrichment in biological processes or pathways using the Ingenuity Pathway Analysis software and the results are presented in Table S10. Interestingly, the top mapped canonical

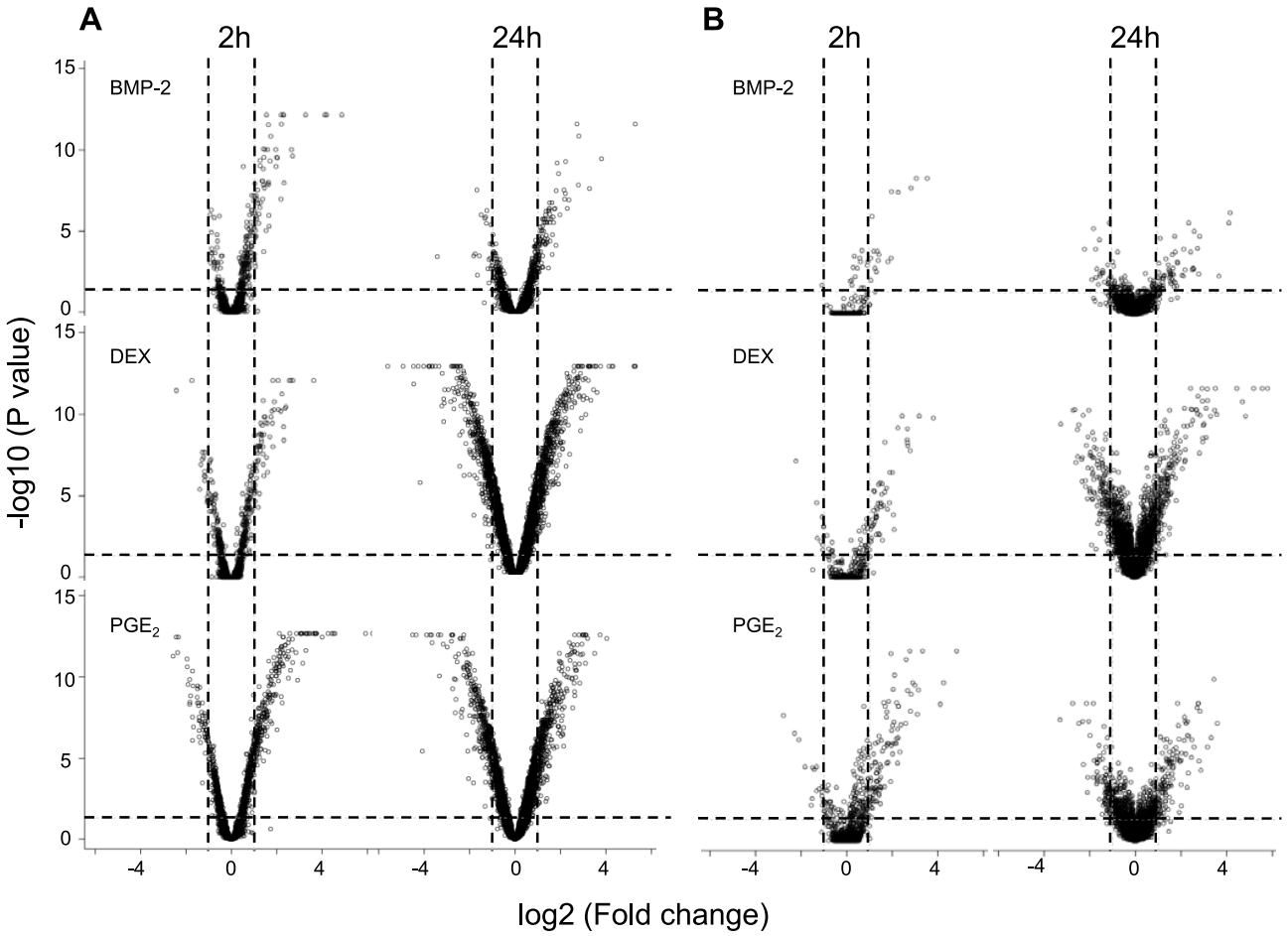

Figure 2. Global response on gene expression upon environmental perturbation. The significance of the treatment-induced effects at two time points, 2h (left panel)and 24h (right panel), on global gene expression assessed by AffymetrixU133+2 arrays (A) and IlluminaRef8 beadarrays (B) in two individuals, respectively, was determined by the Cyber-t test using three biological replicates in BMP-2 (top), DEX (middle) and PGE_2 (bottom) treated versus control samples, respectively. The results from the statistical tests are combined with the magnitude of the change in gene expression following perturbation and visualized in Volcano plots with significance (−log10 P value) versus fold change (log2) on the y – and x-axes, respectively. Lines indicate genes whose expression levels were significantly (FDR adjusted $P<0.05$) changed more than 2-fold.
doi:10.1371/journal.pgen.1001279.g002

pathway for DEX-specific genes is MIF (macrophage migration inhibitory factor)-mediated glucocorticoid regulation (P = 7.43E-04, Fisher's exact test).

We also analyzed the data sets jointly by fitting a linear mixed model where the treatment*SNP interaction term was included and we found similar proportions as above; i.e. at 5% FDR we found a total of 853 *cis*-eQTLs interacting with any treatment compared to 932 at similar FDR using the approach described above (Table S11).

We then sought to validate our top high-confidence DEX-specific *cis*-eQTLs using low-throughput sequencing-based AE assessment [24,25] in samples heterozygous for 1) the top *cis*-eSNP and 2) an intragenic exonic marker either included on the Illumina Hap550K array or imputed from the HapMapII panel. We selected the top five (*MYO6*, *CDSN*, *ZNF480*, *LSM16*, *TMBIM1*) DEX-specific genes (Table 3) where the expression levels were detectable by RT-PCR. *CA2* was excluded due to absence of an exonic marker, and *PLEKHA6* and *USP10* were excluded due to undetected expression in BMP-2 and PGE_2 treated samples, respectively. Of the five selected genes, one failed in sequencing reaction (*CDSN*). Of the remaining four genes we were able to successfully validate treatment specific *cis*-regulation of the *MYO6* locus (Figure 4 and Table S12). Specifically, DEX-treated samples heterozygous for the top eSNP from the *cis*-eQTL analysis (rs646967; DEX eQTL $P = 8.8\times10^{-10}$, BMP-2 eQTL P = 0.8, PGE_2 eQTL P = 0.06; Figure 4A) showed allele-specific expression revealed by differences in RNA (cDNA) allele ratios at the marker heterozygous site. The normalized allele ratio within each DEX-treated sample deviated greater than 2SD from the corresponding BMP-2, PGE_2, and genomic DNA heterozygote ratio, respectively, and we found an overall significant difference in mean $|\Delta$ het ratio$|$ between treatments (rs12606; $|\Delta$ het ratio$|_{DEX} = 0.52\pm0.26$ and $|\Delta$ het ratio$|_{BMP\text{-}2+PGE2} = 0.04\pm0.02$; $P = 2.7\times10^{-4}$, t-test; Figure 4B).

We fine-mapped the candidate region upstream of the *MYO6* gene by including imputed, untyped HapMapII SNPs and found the rs584677 SNP, located ~160kb upstream of the TSS, to have the strongest effect on *MYO6* expression (Figure 4C).

Global impact of perturbation on *cis*-regulation

To directly investigate the impact of environmental perturbation to allelic *cis*-regulation in primary cells, we carried out an independent AE assessment in a subset of five randomly selected samples included in the eQTL study. This was achieved by

Table 1. Summary of results from conditioned *cis*-eQTL analysis in primary cells.

	Untreated (n = 94)	DEX (n = 101)	BMP-2 (n = 96)	PGE_2 (n = 100)
No of SNPs	380,547	380,763	380,069	380,469
No of tests	1,404,011	1,411,793	1,409,707	1,411,346
	No of cis-eQTLs: *All/Independent/Genes*			
$P<3.5\times10^{-8}$	994/233/232	1201/283/282	1409/321/320	1532/356/353
FDR 0.01	2931/682/667	3485/715/692	4416/895/858	4556/878/846
FDR 0.05	4937/1121/1062	5899/1281/1206	7314/1571/1451	7550/1571/1449

doi:10.1371/journal.pgen.1001279.t001

applying a direct method for measuring allele-specific *cis*-regulation in a genome-wide manner as we described recently [26]. The genome-wide AE test was carried out on Illumina HumanOmni1-Quad genotyping chips by interrogating differences in RNA (cDNA) allele ratios at heterozygous sites across primary transcripts normalized to genomic DNA allele ratios from the same individual. All four cell-culture conditions (DEX, BMP-2, PGE_2 and untreated control) were employed in the experiment with the DEX treatment carried out in duplicate, resulting in a total of 25 samples from five individuals included in the analysis. We verified that these newly cultured cells responded to each treatment as expected (Table S13, see Methods). A duplicate DEX and PGE_2 sample failed for one individual leaving a total of 23 AE profiles for analysis. The cDNA data at each heterozygous site were subjected to expression (signal intensity) and allele resolution filters [26], respectively, along with a novel method for normalization of signal intensity induced biases in allele ratio estimates (see Methods).

Initially, we looked for convergence of the AE data with our *cis*-eQTL data. Using five individuals we did not have power to independently map *cis*-rSNPs [26], therefore we focused on samples heterozygous for significant treatment-specific *cis*-eSNPs (defined as being significant in one treatment at 5% FDR and non-significant, $P>0.05$, in all three remaining conditions). In total, 162/485 genes (Table S14) with treatment-specific *cis*-regulation from the eQTL study were informative for AE test, i.e. at least one out of five samples being heterozygous for a *cis*-eSNP and with the region being robustly expressed. We then used windows of three consecutive heterozygous SNPs (at least three of four informative SNPs above signal threshold in each sample) to detect differential allelic expression, defined as an average $|\Delta$ het ratio$|>0.05$ (corresponding to 1.2-fold difference between alleles) among SNPs showing empirical probability of $P<0.05$ (see Methods).

Of the 162 tested regions, evidence of a *cis*-regulatory effect was independently confirmed for 73 (45%) genes (Table S14).

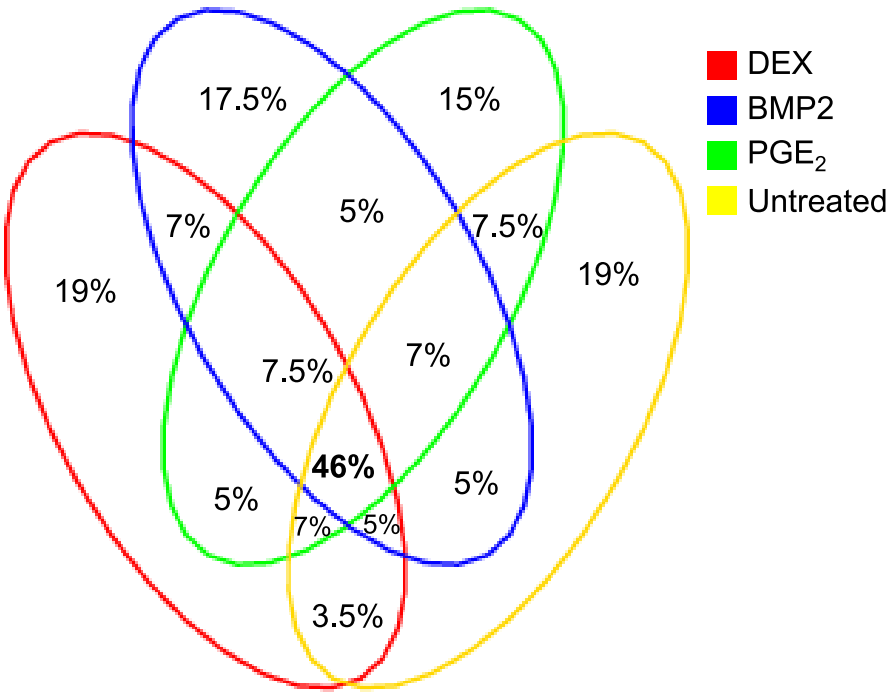

Figure 3. Overlap of significant cis-eQTLs across treatment. Top 3000 *cis*-eQTLs per treatment (FDR<1%) are visualized in a Venn diagram showing the different levels of sharing across treatment.
doi:10.1371/journal.pgen.1001279.g003

Table 2. High-confidence treatment-specific *cis*-eQTLs.

	No of treatment-specific *cis*-eQTLs: *All/Independent/Genes*		
	P<3.5×10^{-8}	**FDR 0.01**	**FDR 0.05**
Untreated	1/0/0	11/6/6	106/77/72
DEX	7/3/3	44/25/25	243/122/121
BMP-2	3/1/1	73/34/33	294/150/143
PGE_2	4/1/1	58/19/19	289/140/134

doi:10.1371/journal.pgen.1001279.t002

However, of these, we were able to confirm treatment-specific effects for only a minority (5 of 73 loci, 7%). For the remaining 68 loci (93%), allele-specific expression was observable across treatments (Table S14). The five validated treatment-specific *cis*-eSNPs were shown to have a greater effect on induced gene expression indicated by differences in fold change (AA versus BB) than the 68 treatment-independent loci (Figure S7).

Next, we used our AE data set to assess the global impact of treatment in allelic *cis*-regulation by measuring AE differences within (for duplicate measurements used in the case of DEX) or between treatments in one individual or across samples. The genome-wide profiles of treatment induced allelic *cis*-variation measured the difference of average allele-ratios [mean($|\Delta$ het ratio$|_{\text{test}} - |\Delta$ het ratio$|_{\text{ref}}$)] using windows of three consecutive heterozygous SNPs in robustly expressed RefSeq regions (at least three of four informative SNPs above signal threshold in both samples). Each treatment (''test'') was correlated to the same DEX (''reference'') sample and only windows expressed in all treatments were used for within individual comparisons. Treatment explained ~10–15% of variance of AE within an individual (r = 0.87–0.89 DEX versus DEX, r = 0.77–0.79 DEX versus other treatment) (Figure 5A). In contrast, the variance of allelic expression among individuals was considerably higher (average r = 0.4), which eliminated any observable difference within (Figure 5B) or between treatments (Figure 5C). Overall, these results reiterate the relative stability of allelic *cis*-regulation upon environmental perturbation within a cell type as observed in our eQTL survey as well as heritability of AE phenotypes observed earlier by us [26] and others [11].

Finally, we explored the possibility of identifying loci accounting for the 10–15% higher variance in *cis*-regulation observed upon perturbation by observing outliers in treatment comparisons within samples. We used three SNP windows where all measurement points consistently showed either lower or higher deviation from equal expression in reference (DEX) versus test samples (BMP-2, PGE_2 or untreated control), with 40K window pairs available on average. Genome-wide distribution of pair-wise differences allowed us to assign a probability (empirical significance) for observing three consecutive SNPs with a certain degree of directional difference (consistently greater or smaller deviation from equal expression in consecutive SNPs) between reference and test sample. On average, window pairs reaching permutation significance of 0.05 or lower (1.8% on average) were further assessed to look for genes with DEX-specific allelic expression differences. We observed 16–84 genes (at 12–25% FDR, see Methods) per sample (Table S15) where DEX treatment consistently differed from all three other cell culture conditions

Table 3. Top high-confidence treatment specific *cis*-eQTLs.

DEX-specific			*BMP-2-specific*			*PGE_2-specific*		
Gene	*SNP*	*eQTL P*	*Gene*	*SNP*	*eQTL P*	*Gene*	*SNP*	*eQTL P*
MYO6	rs646967	8.8E-10	**HSPA2**	rs10498516	8.5E-9	**CSMD1**	rs11782360	1.3E-12
CA2	rs10504814	1.0E-9	**SMARCD2**	rs2665840	4.9E-7	**GJA4**	rs2093880	9.3E-08
PLEKHA6	rs17334002	1.5E-8	**SPSB1**	rs2071931	6.5E-7	**SPINK4**	rs3860974	1.7E-07
CDSN	rs3873334	3.8E-7	**RIOK2**	rs2544771	8.0E-7	**MGC39715**	rs12680064	2.2E-06
USP10	rs16974016	1.9E-6	**CCL15**	rs1634508	9.4E-7	**SIRT6**	rs3760905	2.2E-06
ZNF480	rs321930	3.8E-6	**TTLL11**	rs10818589	1.4E-6	**GLP2R**	rs2277689	4.4E-06
LSM16	rs6495119	4.0E-6	**ZNF354A**	rs11743893	1.6E-6	**SYTL2**	rs290198	4.5E-06
TMBIM1	rs992157	5.2E-6	**NR2C2**	rs9816383	1.7E-6	**LPIN2**	rs661767	4.7E-06
IFT74	rs4878149	6.6E-6	**C21orf6**	rs2832057	1.8E-6	**STARD3**	rs1877031	5.2E-06
TM4SF11	rs2046532	7.9E-6	**COPB2**	rs9289573	3.1E-6	**PCDH18**	rs1320342	5.6E-06
OR1D4	rs2469798	8.9E-6	**C14orf50**	rs10134770	3.2E-6	**KLRK1**	rs2734565	8.7E-06
FLJ32569	rs17433088	9.4E-6	**OR5T3**	rs2512950	3.9E-6	**RGS2**	rs7415619	8.9E-06
MAGI2	rs3779317	1.0E-5	**ABCG4**	rs2511841	5.0E-6	**BLVRA**	rs849165	1.0E-05
WDR66	rs895959	1.6E-5	**C9orf106**	rs3928291	6.3E-6	**SORCS3**	rs10786828	1.1E-05
PACS1	rs3741370	1.6E-5	**ETV2**	rs2312305	7.4E-6	**IFI44L**	rs1033999	1.8E-05
RNF190	rs7226286	1.6E-5	**KIAA0133**	rs2295625	8.2E-6	**SULT1E1**	rs1354360	2.1E-05
OGFOD2	rs883263	1.7E-5	**DTWD2**	rs11740134	8.9E-6	**BLOC1S3**	rs8111069	2.2E-05
SEMA3E	rs1524332	1.8E-5	**HS747E2A**	rs1997719	9.3E-6	**HSPA4**	rs3885730	2.2E-05
ZNF513	rs780090	2.0E-5	**COMMD10**	rs4283832	1.1E-5	**DYNC1I2**	rs6752812	2.2E-05
NRM	rs6911628	2.0E-5	**SOX8**	rs7187700	1.2E-5	**TNFSF11**	rs9533108	2.4E-05

doi:10.1371/journal.pgen.1001279.t003

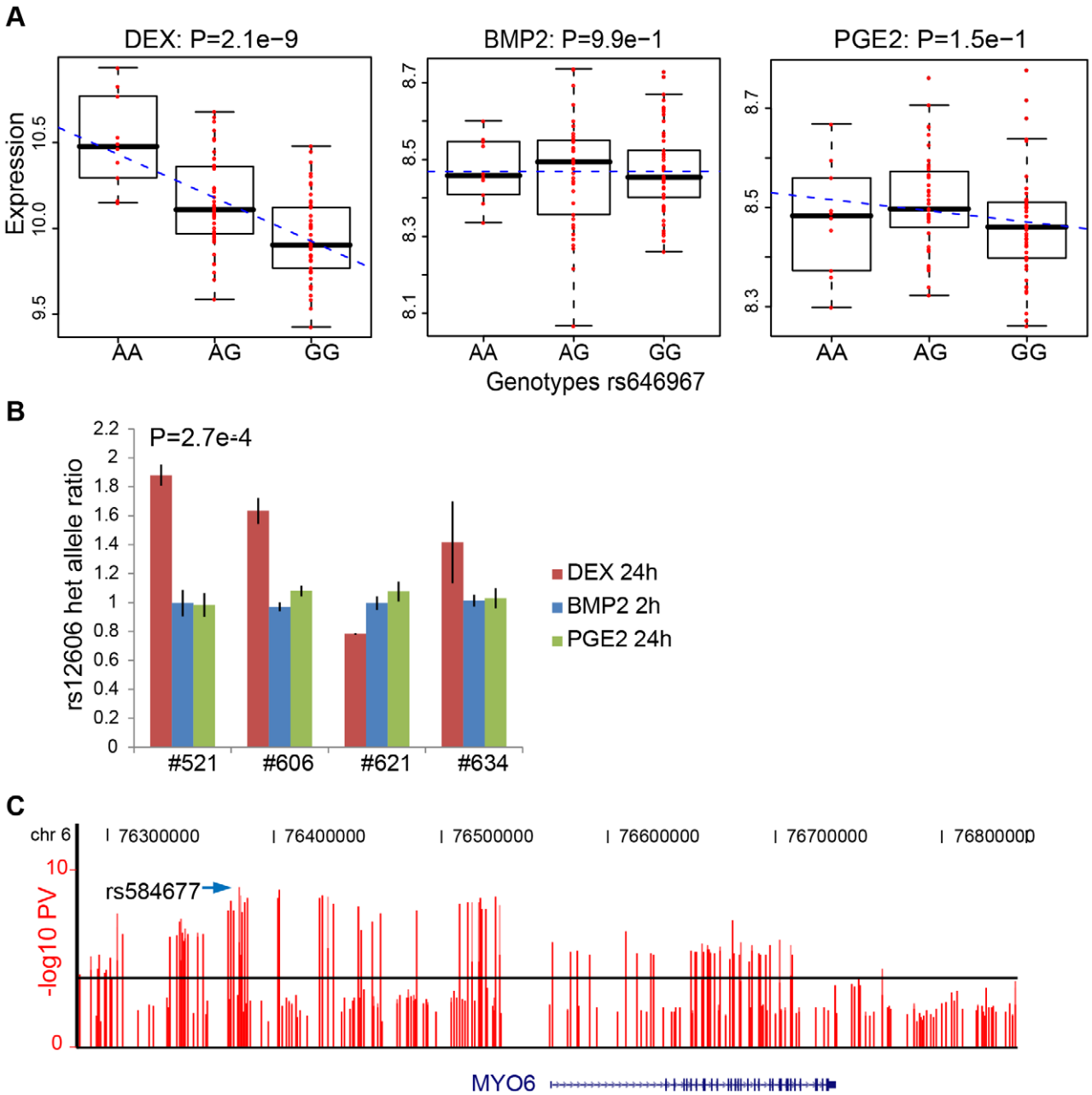

Figure 4. DEX–specific cis-regulation of MYO6 expression. (A) The rs646967 SNP located upstream of the *MYO6* gene was shown to be strongly associated with *MYO6* expression in DEX-treated cells (top left) with no effect in BMP-2 (top middle), PGE-2 (top right) or untreated samples (data not shown). Expression scores from Illumina Ref8 BeadArrays for each individual are averaged from two biological replicates and shown as red circles and the regression line from linear regression model is indicated with blue dashes. (B) The treatment-specific effect of *cis*-regulation of *MYO6* expression was validated by sequencing-based allelic expression test in four samples heterozygous for both the rs646967 *cis*-eSNP and for the intragenic rs12606 marker. Normalized rs12606 heterozygote allele ratios of RNA samples from DEX (24h), BMP-2 (2h) and PGE_2 (24h) treated cells were compared within and between samples and data are presented as mean ± SD of three technical replicates. Significant P-value is obtained from t-test comparing |Δ het ratio| in DEX versus BMP-2 and PGE_2 samples. (C) The *cis*-eQTL analysis of the *MYO6* region was expanded by the inclusion of imputed untyped HapMapII SNPs. The P-values from the linear regression analysis represented as $-\log_{10}$(P-value) are shown as vertical bars with a horizontal line indicating a cutoff of $P=10^{-4}$. The rs584677 SNP, marked with an arrow, located ~160kb upstream of the transcription start site showed the most significant association with *MYO6* expression.
doi:10.1371/journal.pgen.1001279.g004

suggesting a direct interaction between *cis*-variants and environmental perturbation. Notably, these genes were 2.3–6.2-fold more common among the DEX response genes (significant >1.5-fold difference in expression upon DEX induction) (Table S2 and S15) than expected by chance (binomial $P<0.05$ for each sample). These results suggest that specific interaction of *cis*-regulatory sequences with the environment can be directly identified *in vivo* by genome-wide AE measurements.

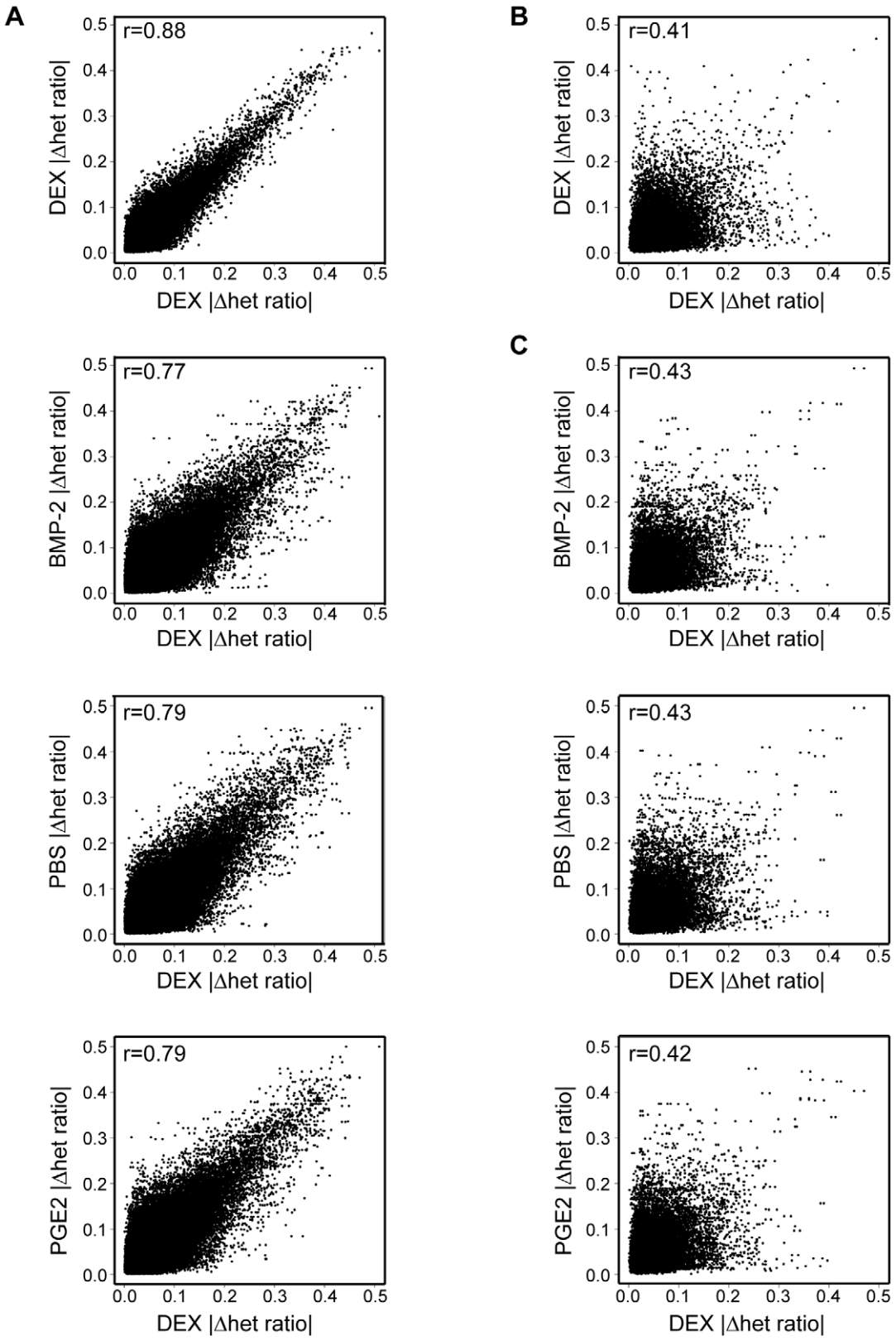

Figure 5. Global effect of environmental perturbation on allelic *cis*-regulation. (A) Treatment specific changes in AE within an individual (left panel). A total of 224,944 expressed three SNP windows measured in both DEX samples and in three other conditions were available across four individuals. The x-axis shows magnitude of AE (|Δhet ratio|) in reference DEX window correlated against magnitude of AE observed in independent DEX measurement on y-axis, against AE observed in BMP-2 treatment, against PBS or PGE2. The Pearson correlation (R) for each pair-wise comparison is shown and demonstrates that treatment contributes slightly to differential *cis*-regulation observed by the genome-wide AE test. (B) Interindividual, treatment independent variation in allelic expression (upper right panel). A total of 27,836 identical informative three SNP windows were measured

between individuals upon DEX treatment. The Pearson R is considerably lower than for within sample comparisons indicating that most of the AE variation between individuals is driven by determinants shared between these cells and independent of treatment. (C) Interindividual, treatment dependent variation in AE (right panel). A total of 159,926 identical informative three SNP windows were available for correlating DEX treatment to any of the three other treatments between individuals. Correlations between individuals across treatments are not significantly different from within treatment correlation between individuals shown in (B), indicating that the treatment specific effects observed within individual (A) are sufficiently weak to be globally unnoticeable due to much stronger correlation of AE to interindividual differences.
doi:10.1371/journal.pgen.1001279.g005

Dexamethasone specific *cis*-regulation of the Tenascin-C (*TNC*) locus—a corticosteroid pharmacogenetic candidate locus

We followed-up and validated our top DEX-dependent *cis*-regulated locus, the Tenascin-C (*TNC*) locus, identified in the global AE test (Figure 6A) using low-throughput methods in an extended set of samples as well as at different time points (t = 2h and t = 24h). We were able to successfully confirm the treatment-specific effect after 24h but no difference in AE was seen after 2h (Figure 6B) indicating a time-dependent effect of the gene regulation.

We extended our *cis*-eQTL analysis in DEX-treated samples by including imputed HapMapII SNPs in order to fine-map the association and found the top SNP (rs7850103, $P = 2\times10^{-7}$) located ~250 kb upstream of the TSS (Figure 6C). Further real-time RT-PCR experiments confirmed that down-regulation of *TNC* expression by DEX is genotype-dependent (Figure S8). We then asked whether DEX-dependent heritable *cis*-regulation of *TNC* expression could underlie the difference in inhaled corticosteroid treatment response in the treatment of childhood asthma. We chose asthma as a clinical model given that (1) inhaled corticosteroids represent the most commonly prescribed and efficacious asthma controller medication; (2) clinical response to inhaled corticosteroids in asthma is variable between subjects; and (3) *TNC* expression is known to be increased in lung tissue of asthmatics, which is modulated by corticosteroid treatment [27]. We tested six SNPs located in our candidate region in children with mild-to-moderate persistent asthma enrolled in a multicenter, randomized, placebo-controlled trial of inhaled anti-inflammatory medication. The analysis was limited to 170 children of self-reported non-hispanic white ancestry randomized to daily, inhaled budesonide treatment, on whom lung function (forced expiratory volume in one second (FEV_1)) had been measured before and after two months of corticosteroid treatment. We found suggestive associations between the *TNC cis*-variants and response to inhaled corticosteroid (rs955387-A, beta = −6.99, P = 0.005; rs10982634-C, beta = −6.01, P = 0.01; rs10817727-G, beta = −5.78, P = 0.02; rs12380804-A, beta = −8.09 P = 0.02; rs10982611-G, beta = −2.87, P = 0.07; rs10817762-C, beta = −2.785, P = 0.08) (Figure 6D) although independent replication is needed to confirm these findings.

Discussion

We have studied how environmental perturbation impacts genetic *cis*-regulation of global gene expression in primary human osteoblasts. To our knowledge, this is the first study exploring the *cis*-regulatory landscape in a population panel of human cells cultured under multiple conditions and time points. Environmental stimuli included growth factors, cytokines and steroid hormones known to be relevant to the cell type studied and with previous known effects on the osteoblast transcriptome [15–21]. The robust response to treatment was verified both within and across samples using different expression platforms and clearly showed evidence of biologically relevant transcript changes such as the significant down-regulation of the IGF1 signaling pathway following glucocorticoid stimulation [14]. However, despite the large impact on the transcriptome by the treatments, we found that only a small proportion of the identified *cis*-eQTLs can be considered as true treatment-specific, indicating that global changes in gene expression may be governed more by subtle heritable and environmental effects.

Our experimental design with the inclusion of multiple independently derived cell lines as biological replicates improved not only the detection of response genes but also the discovery of treatment-specific and treatment-independent *cis*-eQTLs. We have previously shown that by including such replicates, approximately 60% more *cis*-eQTLs can be identified compared to the use of single replicates [7]. Using this design in multiple conditions, we identified ~40% more *cis*-eQTLs in conditioned samples as compared to untreated controls but interestingly, when we compared them across treatments we found that the majority (>90%) of them were seen in more than one condition. These findings were confirmed in a slightly different study design separating the biological replicates and performing two independent *cis*-eQTL analyses per treatment. This indicates that environmental perturbation seems to allow a higher discovery rate of genetic *cis*-effects not because of treatment-specific regulatory variants but rather due to increased power in *cis*-eQTL analysis in conditioning cells, perhaps attributable to a higher level of coordination of gene regulatory activity between treatments (i.e. reducing environmental variability of "resting cell culture").

In contrast to environmental-dependence, cell-type specific *cis*-regulation of gene expression has previously been studied with contrasting results. Using human primary fibroblasts and immortalized B-lymphocytes, Lee et al [11] found that up to 10% of the genes studied might be influenced by tissue-specific *cis*-regulatory variants whereas Dimas et al [4] reported that 69–80% of regulatory variants operate in a cell type-specific manner using similar human cell panels. Notably, the former study utilized AE monitoring and the latter applied eQTL-mapping. Lee et al [11] also explored how *cis*-regulation is affected by experimental conditions following iPS reprogramming, and their results indicated that allele-specific expression remained largely invariable. Our results are consistent with the more conservative estimates of context specificity of *cis*-regulatory variation reported by others [11,28]. In line with this are the recent observations indicating that at genome-wide level, *trans*-variants predominate when hypothesis free mapping of perturbation specific effects are mapped [12,13,29]. Based on our earlier results [7], we chose not to pursue analyses including *trans* variants, since even among biological replicates these cannot be reproduced in the current sample size.

However, we followed-up and validated our findings from the *cis*-eQTL analysis by measuring global allele-specific expression pattern in the different conditioned cells. This allowed us to study treatment-specific *cis*-effects in more detail due to higher sensitivity and specificity of the approach [26]. We were able to validate ~45% of the *cis*-regulatory effects identified in the eQTL analysis which is in fact similar to what has been shown previously comparing AE mapping with traditional *cis*-eQTL mapping [26]. The reason for the remaining 55% of the *cis*-eQTL not being

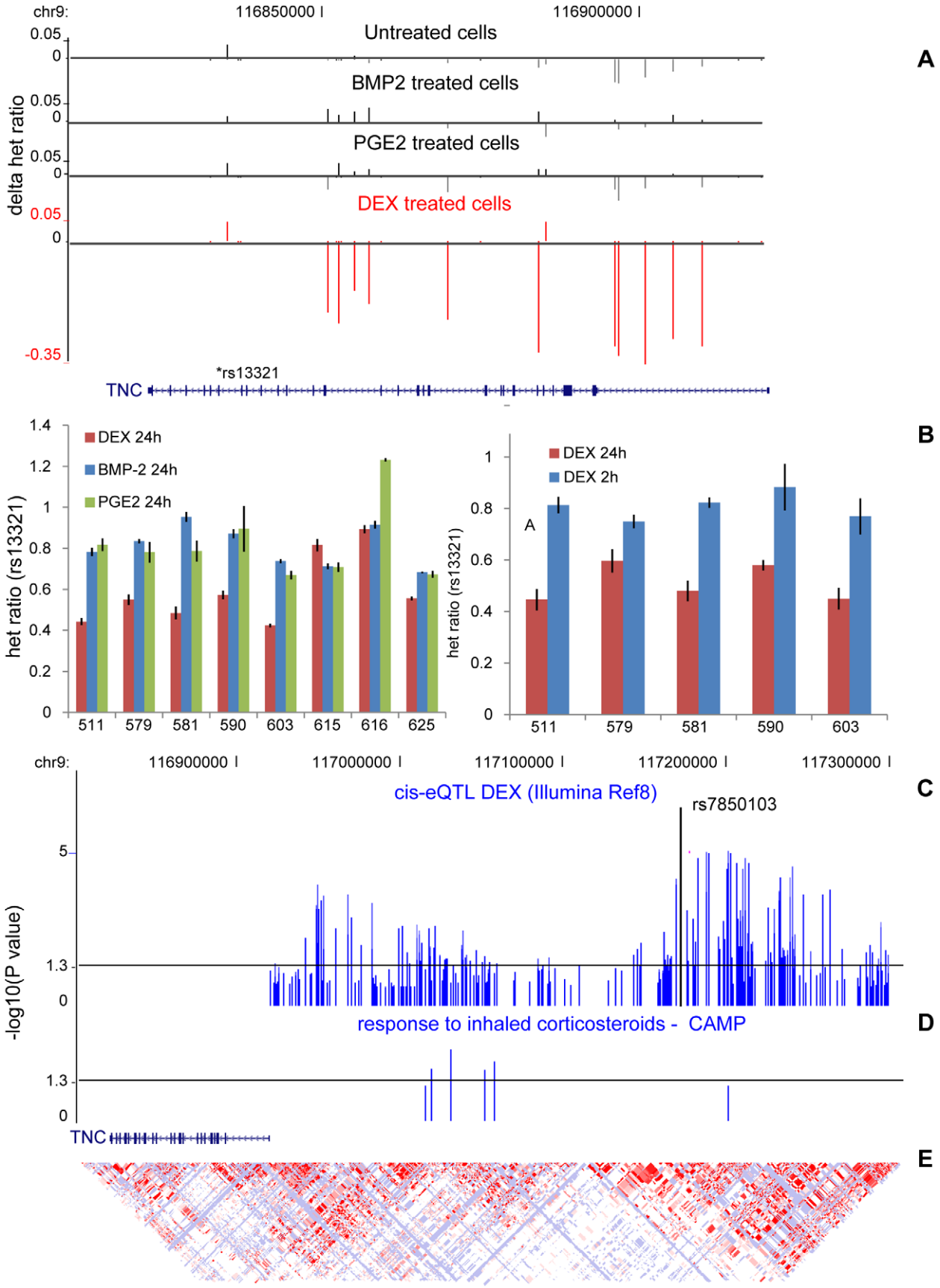
chr9:
116850000
116900000
Untreated cells
BMP2 treated cells
PGE2 treated cells
DEX treated cells
delta het ratio
0.05
0
-0.35
*rs13321
TNC
A
DEX 24h
BMP-2 24h
PGE2 24h
het ratio (rs13321)
511
579
581
590
603
615
616
625
DEX 24h
DEX 2h
A
B
chr9:
116900000
117000000
117100000
117200000
117300000
cis-eQTL DEX (Illumina Ref8)
rs7850103
-log10(P value)
C
response to inhaled corticosteroids - CAMP
D
TNC
E

Figure 6. Time-dependent effect of DEX on *TNC* allelic expression. (A) DEX-specific *cis*-regulation of the Tenascin-C (*TNC*) gene located on chromosome 9 was identified in genome-wide allelic expression (AE) tests by assessing differences in RNA allele ratios at heterozygous sites normalized to genomic DNA allele ratios (Δhet ratio) across the transcripts. The Δhet ratio from AE tests are shown as vertical bars for untreated (black, 1st track), BMP-2 (black, 2nd track), PGE_2 (black, 3rd track) and DEX (red) treated samples. The direction of effect (+/−) is based on phased genotype data in the shown individual and marked deviations from equal expression (Δhet ratio = 0) are observed only in DEX treated (red) sample, which predominantly occur in same allele based on statistical phasing. The relatively overexpressed chromosome in this individual harbors the allele expected to be overexpressed based on population eQTL data (see panel C). (B) The DEX-specific *cis*-effect of the *TNC* locus was validated by sequencing-based AE test in samples heterozygous for the rs13321 exonic marker. Normalized heterozygote allele ratios of RNA samples from DEX (24h), BMP-2 (2h) and PGE_2 (24h) treated cells were compared within and between samples and data are presented as mean ± SD of three technical replicates. In 6/8 DEX-treated samples (red), normalized allele ratio deviated greater than 2SD from genomic DNA heterozygote ratio. Significant P-value ($P = 2.6\times10^{-3}$) was obtained from t-test comparing normalized allele ratio in DEX versus BMP-2 (blue) and PGE_2 (green) samples. Sequencing-based AE test was then repeated in five DEX-treated samples at the earlier time point (2h) but no deviation from genomic DNA heterozygote ratio was shown. Significant P-value ($P = 7.1\times10^{-5}$) was obtained from t-test comparing normalized allele ratio in DEX 24h (red) versus 2h (blue) samples. (C) *cis*-eQTL analysis of the *TNC* locus was performed using genes expression scores IlluminaRef8 array (N = 101). The P-values from the linear regression analysis represented as $-\log_{10}$(P-value) are shown as vertical bars with a horizontal line indicating a cutoff of P = 0.05. The top SNP rs7850103 ($P = 2.3\times10^{-7}$) is marked in the figure. (D) SNPs (n = 6) in the *TNC* candidate region were associated with response to inhaled corticosteroid treatment in 170 children with mild-to-moderate persistent asthma. The P-values from the linear regression analysis represented as $-\log_{10}$(P-value) are shown as vertical bars with a horizontal line indicating a cutoff of P = 0.05. (E) The HapMap Phasell CEU LD blocks are shown as a diamond-shaped plot using log odds (LOD) measures.
doi:10.1371/journal.pgen.1001279.g006

validated can be due to insufficient power in AE test, false positives in eQTL mapping, or measurement of mRNA versus pre-mRNA in eQTL and AE studies, respectively. Nevertheless, the results from these allele-specific expression assessments confirmed our previous findings from eQTL analysis and strengthened the hypothesis that a large proportion of *cis*-regulatory variants are shared across treatments. In fact, the majority of the environmental-dependent regulatory variants that were identified in eQTL analysis were shown to be shared across multiple treatments. The reason for these numerous false-negatives could be explained by the sensitivity of the eQTL approach where identification of *cis*-regulation of low expression transcripts is challenging. An example of this occurrence is the *cis*-acting variant regulating the expression of *TNFSF4* that has been associated with susceptibility to systemic lupus erythematosus and whose *cis*-regulatory effect is largely pronounced in activated cells as compared to non-activated cells due to up-regulation of *TNFSF4* expression upon activation [30].

In addition to validating our findings from *cis*-eQTL analysis, we used the AE assessments to try and further detect environmental-dependent *cis*-regulatory effects, focusing on the DEX treatment. DEX is a synthetic glucocorticoid steroid hormone that regulates gene expression through binding to its nuclear receptor, the glucocorticoid receptor (GR). The ligand-receptor complex binds the DNA at specific glucocorticoid response elements (GRE) resulting in activation or repression of gene expression [31]. Here, we were able to detect on average ~60 genes/sample with evidence of DEX-specific AE differences enriched among DEX-responsive genes (i.e. showed a significant >1.5-fold difference in expression upon DEX stimulation) allowing us to speculate whether the causative eSNP may affect the GR-GRE binding and subsequent the DEX-GR ability to regulate gene expression. Recently a comprehensive ChIP-seq study was presented of DEX-GR binding and its effect on gene expression throughout the human genome [32]. Reddy et al showed that while genes activated with DEX treatment have GR bound in proximity to the TSS, genes repressed with DEX treatment have GR bound >100kb from the TSS. Moreover, another striking difference between genes activated and repressed by DEX was the time required for gene expression response to DEX with repression beginning much later than activation following DEX exposure. Interestingly, these features were seen for our top significant DEX-specific *cis*-regulated locus, the Tenascin-C (*TNC*) locus. Tenascin-C is an extracellular matrix protein whose expression is up-regulated in inflammatory conditions, such as rheumatoid arthritis [33] and asthma [27] and known to be down-regulated by DEX [27,34]. Here we showed that the DEX-specific down-regulation of *TNC* is both genotype- and time-dependent with a significant *cis*-regulatory effect seen only after the later time point of DEX exposure and with the top SNP being located ~250 kb upstream of the TSS. In fact, the same region on chromosome 9 was identified by ChIP-seq to be bound by GR in human A549 lung epithelial carcinoma in response to DEX treatment [32].

In conclusion, our results indicate that qualitative (“on/off”) interactions between controlled environmental perturbation and heritable *cis*-regulatory SNPs are uncommon. Therefore, uncovering true interactions requires either multi-pronged approaches where independent tools are used to assess treatment specificity on genetically controlled expression, as employed here. Alternatively, larger sample sizes with adequate replication in independent cohorts are required for establishing *cis*-regulatory variant – environment interaction, due to much smaller effect sizes than those observed for natural variation in gene expression among populations. At the same time, the existence of validated, genetically controlled, treatment *cis*-specific effects shown here suggests that systematic functional genomic screens may yield a valuable alternative approach for identifying pharmacogenomic biomarkers altering gene regulation [35], often difficult to access in clinical cohorts due to limited sample sizes.

Methods

Ethics statement

All research involving human participants have been approved by institutional review boards (Dnr Ups 03-561, McGill IRB A10-M121-06B) and conducted according to the principles expressed in the Declaration of Helsinki.

Primary cell culture

Human trabecular bone from the proximal femoral shaft was collected from 113 donors (51 female and 62 male donors, respectively) undergoing total hip or knee replacement at the Uppsala University Hospital, Uppsala, Sweden. The bone samples from each donor were thoroughly minced and cultured in three biological replicates. The cells were grown in medium containing α-MEM (SigmaAldrich, Suffolk, UK) supplemented with 2 mmol/l L-Glutamine, 100U/mL penicillin, 100mg/mL streptomycin (National Veterinary Institute of Sweden, Uppsala, Sweden), and 10% fetal bovine serum (SigmaAldrich, Suffolk, UK) at 37°C with 5% CO_2. At 70–80% confluence, the cells were passaged and sub-cultured in 6-well plates (100,000 cells/well) for 12 days. The

culture medium was changed twice weekly. Prior to treatment, the cells were starved for 20h by adding complete cell medium containing 0.5% fetal bovine serum. The cells were then incubated for 2h and 24h with 0.1 μg/ml of rhBMP-2, 100 nM of dexamethasone, 100 nM of IGF-1, 1μM of PGE2, 100 nM of PTH (1–34), 0.1 nM of TNF-α, 100 nM of 1.25 VitD3 and with the same concentration of control, respectively (Table S16). At the two time points, the cell medium was removed and the cells were harvested by adding 600μL of RLT buffer (Qiagen, GmbH, Germany). The cell lysates were homogenized by using QIAshredder (Qiagen, GmbH, Germany) homogenizers and stored in −70°C until RNA extraction.

The study was approved by the local ethics committees (Dnr Ups 03-561, McGill IRB A10-M121-06B).

RNA extraction

RNA was extracted from cell lysates using the RNeasy Mini Kit (Qiagen, Mississauga, Canada). High RNA quality was confirmed for all samples using the Agilent 2100 BioAnalyzer (Agilent technologies, Palo Alto, CA, USA) and the concentrations were determined using NanoDrop ND-1000 (NanoDrop Technologies, Wilmington, DE, USA).

Expression profiling—Affymetrix GeneChip

Expression profiling of one complete sample was performed in triplicate (biological replicates) using the Affymetrix Human Genome U133 plus 2.0 Array (Affymetrix, Santa Clara, CA, USA). One microgram of RNA was reverse transcribed into cDNA and in vitro transcription was performed to generate biotin-labeled cRNA for subsequent hybridization. Hybridized target cRNA was then stained with streptavidin phycoerythrin, and arrays were scanned using a GeneArray Scanner at an excitation wavelength of 488nm. The raw data was imported to BioConductor [36] using the R 2.5.0 package and normalized mean expression values were generated by the Robust Multichip Average algorithm [37,38].

The microarray data have been deposited in the Gene Expression Omnibus (GEO), www.ncbi.nlm.nih.gov/geo (accession no. GSE10311).

Expression profiling—Illumina BeadChips

Expression profiling of one complete sample and of all BMP-2 (2h, n = 101), dexamethasone (24h, n = 106), PGE_2 (24h, n = 105) and untreated control (24h, n = 95) samples, each with at least two biological replicates, was performed using the Illumina HumRef-8v2 BeadChips (Illumina Inc. San Diego, CA, US) where 200ng of total RNA was processed according to the protocol supplied by Illumina. The raw data was imported to BioConductor [36] using the R 2.5.0 lumi package for variance-stabilizing transformation and robust spline normalization to obtain normalized mean expression values. The detectionCall algorithm in the lumi package was used to find genes uniquely expressed in one condition. A gene was considered expressed if present in at least 10% of the measured samples.

The microarray data has been deposited in the Gene Expression Omnibus (GEO), www.ncbi.nlm.nih.gov/geo (accession no. GSE 15678, GSE21410, GSE21725, GSE21726, GSE21727).

Gene network and pathway analysis

In order to visualize whole-genome expression data in the context of biological networks, functions or pathways data were analyzed through the use of Ingenuity Pathway Analysis (IPA) system (Ingenuity Systems, Mountain View, CA, USA, www.ingenuity.com). The datasets containing differently expressed genes (FDR adjusted $P<0.05$ and Fold change >2) or genes harboring a treatment-specific *cis*-eQTL were uploaded to the application. Each gene identifier was mapped to its corresponding gene object in the Ingenuity Pathways Knowledge Base. A fold change cutoff was set to identify genes whose expression was significantly differentially up or down-regulated. These genes, called Focus Genes, were overlaid onto a global molecular network developed from information contained in the Ingenuity Pathways Knowledge Base. Networks of these Focus Genes were then algorithmically generated based on their connectivity.

The Functional Analysis identified the biological functions that were most significant to the dataset. Genes from the dataset that met the cutoff and were associated with biological functions in the Ingenuity Pathways Knowledge Base were considered for the analysis. Fisher's exact test was used to calculate a p-value determining the probability that each biological function assigned to the dataset is due to chance only.

Assessment of differently expressed genes

The Cyber-t test was used to determine the significance between the observed differences in gene expression. The Cyber-t test is based on simple t-tests and uses the observed variance of gene measurements across replicate experiments, thereby accommodating noise, variability, and low replication, often typical of microarray data [39]. Since the number of tests (genes) is large, the p-values are adjusted for multiple comparisons using the false discovery rate (FDR) algorithm [40] in Bioconductor using the R 2.5.0-package [36].

For the proportion of differentially expressed genes among all tested genes for each treatment (1-pi0) the qvalue package implemented in R was used [40].

DNA extraction

DNA was successfully extracted from cell lysates of 109/113 samples and re-suspended in 200μl PBS using the GenElute DNA Miniprep Kit (SigmaAldrich, Suffolk, UK). Concentrations were determined using the Quant-iT PicoGreen kit (Molecular Probes).

Whole-genome genotyping

Genotyping was performed on 106 samples using the Illumina HapMap 550k Duo chip (Illumina Inc., San Diego, CA, US) according to the protocol provided by the manufacturer. The total number of SNPs included on the chip is 561,303. Individuals with low genotyping rate (<90%) and SNPs showing significant deviation from Hardy-Weinberg equilibrium ($P<0.05$) were excluded. Similarly, low frequency SNPs (MAF<0.10) and SNPs with high rates of missing data (>5%) were excluded. The average success rate of the genotyping of the 561,303 SNPs across all individuals was 99%.

Genotype–phenotype association analysis

Of the 22,184 Illumina probes (corresponding to 18,144 genes), those with SNPs (dbSNP build 126) within them were excluded. We tested for association of the induced expression levels to SNPs using the linear regression model implemented in the PLINK software (http://pngu.mgh.harvard.edu/purcell/plink/) [41] assuming additive effect of the SNPs. Two covariates were also included in the regression model; year of birth and sex ($mRNA = a+b_1SNP_1+b_2cov1_2+b_3cov2_3+e$). *Cis*-regulatory effects were tested using SNPs mapping ±250kb flanking the gene or within the gene itself. In order to study whether array hybridization time point (i.e. batch) biased our data and masked

weak treatment-specific effects we also analyzed the data including batch as a cofactor in exactly overlapping samples across treatments (n = 80) keeping the biological replicates separate in independent *cis*-eQTL analyses.

We also analyzed the data sets jointly by fitting a linear mixed model using the SAS 9.1 software (SAS institute Inc., Cary, NC, US). Treatment group was included as a random effect and year of birth and sex as fixed effects. Two interactions terms were also included; treatment*SNP and sex*SNP, respectively. No significant sex*SNP interaction effects were found.

Independent *cis*-eQTLs were identified by first obtaining genome-wide recombination hotspot coordinates based on the HapMap Phase 2 (release 22, NCBI 36) data (http://hapmap.ncbi.nlm.nih.gov/downloads/recombination). Within each locus we first identified top associations within each interval between recombination hotspots and retained the top ranking association. Next we tested for potential residual LD ($D'>0.5$) between significant associations mapping to independent recombination hotspot intervals in our population using our genotyping as input in the Haploview software (version 4.2) (www.broadinstitute.org/haploview). Only the top association from SNPs showing pairwise $D'>0.5$ was kept for each locus to identify unique *cis*-eQTLs.

Genotype imputation

Genotypes from 103 samples that passed quality control were imputed for all SNPs (n = 478,805) oriented to the positive strand from phased (autosomal) chromosomes of the HapMap CEU Phase II panel (release 22, build 36). Untyped markers were inferred using algorithms implemented in MACH 1.0 [42,43]. R^2 was used as imputation quality control metrics and estimates the squared correlation between imputed and true genotypes. A cut-off of $R^2<0.3$ was used to remove poorly imputed markers. Association of imputed genotypes using estimated genotype probabilities with expression traits was performed using a linear regression model implemented in the MACH2QTL software [42–44] with sex and year of birth as covariates.

The genomic DNA data collected in parallel from 1.1 M SNPs in these individuals also allowed us to measure imputation accuracy across the dataset using a common set of 636,676 SNPs. Overall, 88% of the HapMap SNPs were imputed at 100% accuracy across samples and the error rate within a sample was 3% which is similar to what has been reported previously [45].

Primer design

Primers were designed using the Primer3 v. 0.4.0 software (http://frodo.wi.mit.edu/) and all primer sequences can be found in Table S17.

Sequencing-based AE analysis

Allele-specific expression was assessed by quantitative sequencing [24]. High-quality RNA was used to synthesize first strand cDNA with random hexamers (Invitrogen, Burlington, Canada) and Superscript II reverse transcriptase (Invitrogen, Burlington, Canada). For each locus, we designed exonic primers and we used PeakPicker v.2.115 with the default settings to quantify the relative amount of the two alleles at the heterozygote site measured from the chromatogram after peak intensity normalization. The normalized heterozygote ratios of genomic DNA samples were used to calculate mean and SD for each SNP. If all heterozygote ratios from three technical replicates showed concordant deviation greater than two SDs from the genomic DNA heterozygote ratio mean, the sample was called to have allele-specific expression.

Retroviral transduction of primary osteoblasts

The PA317-neo packaging cells (ATCC Inc, Manassas, VA, US) expressing pLXSN hTERT and pLXSN HPV16-E7 were kindly provided by Dr Eric Shoubridge (McGill University, Montreal, QC, CA). The packaging cells were grown to near confluence in DMEM containing 10% FBS (SigmaAldrich, Suffolk, UK). After 24 h to 48h, the medium containing retroviral particles was harvested and filtered through a 0.45-µm filter and mixed with complete cell medium. Polybrene was added to a final concentration of 4ug/mL.

Five of the cultured human osteoblast lines (see above) were plated in 75-cm^2 culture flasks and cultured in α-MEM (SigmaAldrich, Suffolk, UK) supplemented with 2 mmol/l L-Glutamine, and 10% fetal bovine serum (SigmaAldrich, Suffolk, UK). When cells reached 30–40% confluence, the media were removed and 6 ml of fresh prepared retroviral suspension (1.5 ml of hTERT suspension, and 1.5 ml of E7 suspension and 3 ml of medium, respectively) was added to the cells and incubated 1–2 hours at 37°C. Growth medium was then added with polybrene to bring up to usual flask volume and maintain incubating overnight at 37°C. The media were then removed and the cells were rinsed once with fresh medium and new culture medium without polybrene was added. After 48h, the media were changed to selection media containing 400µg/ml of G418 (Invitrogen, Burlington, ON, CA) and the cells were cultured under these selection conditions for 2–3 weeks.

The immortalized osteoblasts were seeded in 75-cm^2 and cultured in complete cell medium. At 80% confluence, the cells were starved for 20h by adding complete cell medium containing 0.5% fetal bovine serum (SigmaAldrich, Suffolk, UK). The cells were then incubated with 10^{-4} mg/ml of rhBMP-2 (2h), 10^{-7} M of dexamethasone (24h) and 10^{-6} M of PGE2 (24h) and with the same concentration of control, respectively. At the different time points, the cell medium was removed and the cells were harvested by adding 2mL of TRIzol Reagent (Invitrogen, Burlington, ON, CA) and stored in −70°C until RNA extraction.

Robust responses to each treatment of these newly cultured cells were confirmed by comparison of gene expression assessed by real-time RT-PCR experiments in both immortalized and the corresponding primary treated HObs, respectively. Genes validated were selected from expression profiling using the Illumina Ref8 Beadarrays of primary cells.

Real-time RT-PCR

Aliquots of the different RNA from the primary or immortalized cell, respectively, were each annealed to 500 ng of random hexamers (Invitrogen Corporation, Carlsbad, CA, USA) at 70°C in 10 min. First-strand cDNA synthesis was performed using SuperScript II reverse transcriptase (Invitrogen Corporation, Carlsbad, CA, USA) according to manufacturer's instructions.

The target gene as well as the *18S* housekeeping gene were analyzed in triplicates as well as a calibration curve from a two-fold dilution series of control cDNA and non-template control (NTC) samples. The real-time PCR assays were performed on the Rotor-Gene™ 6000 real-time rotary analyzer (Corbett Life Sciences, Sydney, Australia) using the Platinum SYBR Green qPCR SuperMix-UDG (Invitrogen Corporation, Carlsbad, CA, USA) according to manufacturer's recommendation. The cycling conditions on the Rotor-Gene™ 6000 real-time rotary analyzer were: 4 minutes at 95°C, 40 cycles x (20 seconds at 95°C, 30 seconds at 58°C and 30 seconds at 72°C) followed by the dissociation protocol at 72°C.

Results of the experimental samples were analyzed using the comparative C_T method. The C_T mean and standard deviation

value of each technical replicate sample was calculated and the mean C_T value was then normalized to the 18S mean C_T value. All statistical analyses for the associations of delta C_T values with genetic variants were performed using a general linear model in SAS 9.1 (SAS institute Inc., Cary, NC, US).

RNA and DNA preparation for Illumina Human omni1-quad BeadArrays

Approximately 150μg of total RNA was extracted from the cells using the commercially available TRIzol reagent protocol (Invitrogen, Burlington, ON, CA) and subsequently treated with 18 U DNaseI (Ambion Inc., Austin, TX, USA) for 30 min at 37°C and further extracted with phenol/chloroform. High RNA quality was confirmed for all samples using the Agilent 2100 BioAnalyzer (Agilent Technologies, Palo Alto, CA, USA) and the concentrations were determined using the NanoDrop ND-1000 (NanoDrop Technologies, Wilmington, DE, USA). Poly(A) RNA was then isolated using the MicroPoly(A)Purist protocol (Ambion Inc., Austin, Tx, USA) and poly-A enriched RNA quality and quantity was measured using the Agilent 2100 BioAnalyzer and NanoDrop ND-1000, respectively.

DNA from the cell lysates was extracted using the GenElute DNA Miniprep Kit (SigmaAldrich) according to the protocol provided by the manufacturer and concentrations were determined using the NanoDrop ND-1000.

First- and second-strand cDNA synthesis

Approximately 1μg poly-A enriched RNA was annealed to 50ng of random hexamers (Invitrogen, Burlington, ON, CA) at 70°C for 10 min. First- and second strand cDNA synthesis was performed using the Superscript Double-Stranded cDNA Synthesis Kit (Invitrogen, Burlington, ON, CA) according to the manufacturer's instructions. The double-stranded cDNA was extracted with phenol:chloroform:isoamyl alcohol and dissolved in 12ul DEPC-treated water. The size distribution of the double-stranded cDNA samples (average 1.2–1.5kb) was confirmed using the Agilent BioAnalyzer DNA Kit.

Genotyping and AE analysis on Illumina Human omni1-quad BeadChips

Approximately 200ng of genomic DNA and 50–300ng double-stranded cDNA sample was used for the parallel genotyping and AE analysis on the Illumina Infinium Omni1-Quad BeadArrays according to the manufacturer's instructions (Illumina Inc., San Diego, CA, US). Genotypes in genomic DNA were extracted using BeadStudio. The parallel assessment of genomic DNA and cDNA heterozygote ratios was carried out essentially as described earlier [26], but signal intensity normalization at heterozygous sites followed a slightly modified approach. For AE analysis we utilized the X_{raw} and Y_{raw} signal intensities and since the variances in the two channels are not same (i.e. it is a function of total intensity from both channels) we need to correct this variation through normalization to allow comparison between gDNA and cDNA allele ratios. In this study, we only normalized β ratio ($X_{raw}/(X_{raw}+Y_{raw})$) from heterozygous SNPs with total intensity ($X_{raw}+Y_{raw}$) higher than the threshold value of 3000. The scatter plot of β ratio against the logarithm 10 scaled total intensity fits well with polynomial regression model (quadratic regression model). This model shows better fitting than linear regression model we employed earlier for normalization [26], which works well in higher intensity part, but poor in lower intensity part in many samples. The normalization process can be briefly summarized to following steps: 1) The β ratio is calculated along with total intensity in log10 scale for all heterozygous SNPs. 2) All data points with greater than 3000 in total intensity are divided into 50 intensity bins. 3) A fitted curve from the median β ratio in each bin is computed using a polynomial regression model (quadratic regression) $y = b_1x+b_2x^2+a$ where y is expected β ratio from the curve and x is log10 scaled total intensity. 4) From the fitted curve, the expected β ratio based on total intensity calculated. 5) The final normalized β ratio equals ($\beta_{obs}-\beta_{expected}+0.5$). Following normalization, all median β ratio values in all intensity bins should be close, if not equal, to 0.5.

Empirical probabilities for observing differences in AE for transcripts were assessed by first observing the genome-wide distribution of AE-magnitude at expressed heterozygous sites [$\Delta_{het\ \ ratio} = X_{DNA}/(X_{DNA}+Y_{DNA})-X_{RNA}/(X_{RNA}+Y_{RNA})$]. The use of AE magnitude alone allows us to do the comparisons in unphased chromosomes, which we chose to use as a global test since statistical phasing introduces potential errors. However, in case of *TNC* (Figure 6A), we used derived phased [46] data to show that significant biases at individual sites are observed for the same expressed allele. We defined three SNP expressed windows by requiring that at least three of four consecutive heterozygous sites showed signal above threshold. We note that in comparison across treatments, we used only multi-SNP windows that were above signal threshold in all treatments within an individual. This restricted the analysis to 6791/8097 informative RefSeq genes and captured all informative genes (n = 2880) showing above median expression scores based on Illumina Ref-8 data used in eQTL analysis. Multiplicative likelihood of observing three consecutive SNPs with high $\Delta_{het\ ratio}$ magnitude was compared to 5th percentile of multiplicative likelihood in randomly permuted data from same sample. The same process was used in assessing empirical probability of observing DEX-specific changes in allelic expression, except that direction of effect (greater or lower $\Delta_{Dexa\ het\ ratio}$) was taken into account for the three consecutive SNPs and we applied the following formula to calculate $\Delta_{Dex\ het\ ratio} = X_{RNA\_DEX}/(X_{RNA\_DEX}+Y_{RNA\_DEX})-X_{RNA\_OTHER}/(X_{RNA\_OTHER}+Y_{RNA\_OTHER})$. The gene-based false discovery rate (FDR) of DEX-specific AE was also empirically assessed for each sample using RefSeq annotated genes where multiple three SNP windows had been independently measured for same transcript and the empirical FDR represents the proportion of discordant calls among all genes from same sample.

CAMP cohort association analyses

Association between *TNC* SNPs and clinical response to inhaled corticosteroids was performed using information from subjects participating in the Childhood Asthma Management Program (CAMP). CAMP is a multicenter, randomized, double-blind, placebo-controlled trial to investigate the long-term effects of inhaled anti-inflammatory medication (budesonide 200 μg twice daily or nedocromil 8 mg twice daily both versus placebo) in children 5 to 12 years of age. 1,041 asthmatic children were followed for a mean 4.6 years. Trial design and primary outcomes have been published [47]. Individuals were randomized to budesonide, nedocromil, or placebo. Of the non-Hispanic white CAMP probands randomized to inhaled corticosteroids, 118 subjects and their parents were genotyped on the Illumina HumanHap550v3 BeadChip [48], with an additional 52 trios genotyped on the Illumina Human 610-Quad BeadChip. All CAMP subjects provided assent and their legal guardians consent to study protocols and ancillary genetic testing. The two month change in FEV_1 in response to inhaled corticosteroids was calculated as previously described and was shown to be normally distributed [49]. Association between *TNC* SNPs common to both genotyping platforms and inhaled steroid response was calculated

using PLINK [41]under the assumption of an additive model and adjusted for non-genetic covariates including sex, height and age.

Supporting Information

Figure S1 Global response on gene expression upon environmental perturbation. The significance of the treatment-induced effects at two time points, 2h (left panel) and 24h (right panel), on the global gene expression assessed by AffymetrixU133+2 arrays (A) and IlluminaRef8 beadarrays (B) in two individuals, respectively, was determined by the Cyber-t test using three biological replicates in 1.25VitD3 (top), IGF-1 and PTH (middle) and PGE_2 (bottom) treated versus control samples, respectively. PTH failed in IlluminaRef8 expression profiling experiment and thus not included in (B). The results from the statistical tests are combined with the magnitude of the change in gene expression following perturbation and visualized in Volcano plots with significance ($-$log2 P value) versus fold change (log2) on the y – and x-axes, respectively. Lines indicate genes whose expression levels were significantly (FDR adjusted $P<0.05$) changed more than 2-fold.
Found at: doi:doi:10.1371/journal.pgen.1001279.s001 (0.31 MB PDF)

Figure S2 Validation of PGE_2 responsive genes by real-time RTPCR. The effect of 1μM of PGE_2 on gene expression in primary human trabecular bone cells was verified by quantitative real-time (RT) PCR. The same sources of total RNA used in the microarray experiments were used for the data validation. For each gene in the RT-PCR assay, the three biological replicates were analyzed in duplicates and normalized to the 18s mean value. The fold changes between control samples (grey bars) and PGE_2 induced samples (black bars) were calculated using the relative standard curve method. Data are presented as mean and standard deviation.
Found at: doi:doi:10.1371/journal.pgen.1001279.s002 (0.05 MB PDF)

Figure S3 Correlation of expression changes upon treatment between experiments. The expression changes upon BMP-2, dexamethasone and PGE_2 treatment assessed by Affymetrix U133+2 arrays was verified in the whole study population using Illumina HumanRef8 v2 arrays. In total of 13,030 RefSeq genes overlapped the two studies and expression changes of those genes were included in correlation analysis. Fold changes (log2) were calculated using three biological replicates of a single sample from Affymetrix U133+2 arrays and plotted on the y-axis against median fold changes (log2) in the whole study population using Illumina HumanRef8 v2 arrays on the x-axis.
Found at: doi:doi:10.1371/journal.pgen.1001279.s003 (1.30 MB PDF)

Figure S4 Proportion of the variability accounted for by the *cis*-variants. Graphical representation of the proportion of the total variance (R^2, *x-axis*) explained by each independent *cis*-eSNP at 5% FDR. Total number of significant *cis*-eQTLs were 1121 (A-untreated samples), 1281 (B-DEX-treated samples), 1571 (C-BMP-2-treated samples) and 1571 (D-PGE_2-treated samples), respectively.
Found at: doi:doi:10.1371/journal.pgen.1001279.s004 (0.08 MB PDF)

Figure S5 Distribution of independent *cis*-eQTLs around TSS. Graphical representation of the distance (*kb*, *x-axis*) of each independent *cis*-association (5% FDR) relative to the transcription start site (TSS). Total number of significant *cis*-eQTLs were 1121 (A-untreated samples), 1281 (B-DEX-treated samples), 1571 (C-BMP-2-treated samples) and 1571 (D-PGE_2-treated samples), respectively.
Found at: doi:doi:10.1371/journal.pgen.1001279.s005 (0.07 MB PDF)

Figure S6 P-value distribution of treatment-specific eQTLs. Significant dexamethasone-specific *cis*-eQTLs at 1% FDR (n = 3485) were selected and the distribution of corresponding P-value from *cis*-eQTL analysis in BMP-2 (A), PGE2 (B) and untreated samples (C) were displayed in a histogram where tabulated frequencies of cis-eQTLs at each P-value interval are shown as bars.
Found at: doi:doi:10.1371/journal.pgen.1001279.s006 (0.09 MB PDF)

Figure S7 Validated treatment-specific effect on cis-regulation of gene expression. The expression differences in AA versus BB samples (log2 fold change, y-axis) were compared between validated treatment-specific (n = 5, group 1–2) and treatment-independent (n = 68, group 3–4) loci. Group 1 and 3 represent genotype-dependent effect by a specific treatment (BMP-2, dexamethasone or PGE_2) identified in *cis*-eQTL analysis and group 2 and 4 of the averaged effect of the three corresponding treatments for each specific locus, respectively. Results are presented in box plots with a horizontal line in each box representing the median.
Found at: doi:doi:10.1371/journal.pgen.1001279.s007 (0.06 MB TIF)

Figure S8 Time-dependent effect of DEX on TNC allelic expression. Normalized *TNC* expression (deltaCT) in untreated ($P = 0.5$) and DEX-treated samples ($P = 3.7\times10^{-4}$) (left and middle) as well as the fold change ($P = 3.7\times10^{-4}$) (right) was associated with *TNC* rs7859920 genotypes in a linear regression model.
Found at: doi:doi:10.1371/journal.pgen.1001279.s008 (0.92 MB EPS)

Table S1 Proportions of differently expressed genes (1-pi0) using Storey's q value.
Found at: doi:doi:10.1371/journal.pgen.1001279.s009 (0.02 MB XLS)

Table S2 Response genes following DEX stimulation for 24h.
Found at: doi:doi:10.1371/journal.pgen.1001279.s010 (3.73 MB XLS)

Table S3 Response genes following BMP-2 stimulation for 2h.
Found at: doi:doi:10.1371/journal.pgen.1001279.s011 (3.73 MB XLS)

Table S4 Response genes following PGE_2 stimulation for 24h.
Found at: doi:doi:10.1371/journal.pgen.1001279.s012 (3.73 MB XLS)

Table S5 Summary of results from two independent *cis*-eQTL analyses separating the biological replicates.
Found at: doi:doi:10.1371/journal.pgen.1001279.s013 (0.02 MB XLS)

Table S6 Summary of independent *cis*-eQTLs at 5% FDR.
Found at: doi:doi:10.1371/journal.pgen.1001279.s014 (0.89 MB XLS)

Table S7 DEX-specific *cis*-eQTLs at 5% FDR.
Found at: doi:doi:10.1371/journal.pgen.1001279.s015 (0.34 MB XLS)

Table S8 BMP-2-specific *cis*-eQTLs at 5% FDR.

Found at: doi:doi:10.1371/journal.pgen.1001279.s016 (0.39 MB XLS)

Table S9 PGE_2-specific *cis*-eQTLs at 5% FDR.
Found at: doi:doi:10.1371/journal.pgen.1001279.s017 (0.09 MB XLS)

Table S10 Gene enrichment analysis.
Found at: doi:doi:10.1371/journal.pgen.1001279.s018 (0.03 MB XLS)

Table S11 Significant SNP*treatment interactions.
Found at: doi:doi:10.1371/journal.pgen.1001279.s019 (0.06 MB XLSX)

Table S12 Treatment-specific *cis*-eQTLs validated in sequenced-based AE test.
Found at: doi:doi:10.1371/journal.pgen.1001279.s020 (0.02 MB XLS)

Table S13 Treatment response in primary versus immortalized cells.
Found at: doi:doi:10.1371/journal.pgen.1001279.s021 (0.02 MB XLS)

Table S14 Treatment-specific *cis*-eQTLs validated in global AE test.
Found at: doi:doi:10.1371/journal.pgen.1001279.s022 (0.09 MB XLS)

Table S15 DEX-specific AE.
Found at: doi:doi:10.1371/journal.pgen.1001279.s023 (0.03 MB XLS)

Table S16 Description of treatment panel.
Found at: doi:doi:10.1371/journal.pgen.1001279.s024 (0.03 MB XLS)

Table S17 Primer sequences.
Found at: doi:doi:10.1371/journal.pgen.1001279.s025 (0.02 MB XLS)

Acknowledgments

The authors thank research nurses and assistants, especially Jessica Pettersson and Anna-Lena Johansson, at the Departments of Surgical and Medical Sciences, Uppsala University, Sweden, for large-scale collection and culture of bone samples. We also thank Professor Eric Shoubridge (Montreal Neurological Institute, McGill University, Canada) who kindly provided retroviral vectors and Timothy Jones (McGill University, Montreal, Canada) for culture of packaging cell lines.

We thank all CAMP subjects for their ongoing participation in this study. We acknowledge the CAMP investigators and research team for collection of CAMP Genetic Ancillary Study data. All work on data collected from the CAMP Genetic Ancillary Study was conducted at the Channing Laboratory of the Brigham and Women's Hospital under appropriate CAMP policies and human subject protections.

Author Contributions

Conceived and designed the experiments: EG STW KT BAR TP. Performed the experiments: EG VA BG QLD KCLL VK STW KT. Analyzed the data: EG VA TK BG QLD AK TP. Contributed reagents/materials/analysis tools: AK STW KT HM BAR ON TP. Wrote the paper: EG VA TK QLD STW BAR TP.

References

1. Dixon AL, Liang L, Moffatt MF, Chen W, Heath S, et al. (2007) A genome-wide association study of global gene expression. Nat Genet 39: 1202–1207.
2. Kwan T, Benovoy D, Dias C, Gurd S, Provencher C, et al. (2008) Genome-wide analysis of transcript isoform variation in humans. Nat Genet 40: 225–231.
3. Stranger BE, Nica AC, Forrest MS, Dimas A, Bird CP, et al. (2007) Population genomics of human gene expression. Nat Genet 39: 1217–1224.
4. Dimas AS, Deutsch S, Stranger BE, Montgomery SB, Borel C, et al. (2009) Common regulatory variation impacts gene expression in a cell type-dependent manner. Science 325: 1246–1250.
5. Emilsson V, Thorleifsson G, Zhang B, Leonardson AS, Zink F, et al. (2008) Genetics of gene expression and its effect on disease. Nature 452: 423–428.
6. Goring HH, Curran JE, Johnson MP, Dyer TD, Charlesworth J, et al. (2007) Discovery of expression QTLs using large-scale transcriptional profiling in human lymphocytes. Nat Genet 39: 1208–1216.
7. Grundberg E, Kwan T, Ge B, Lam KC, Koka V, et al. (2009) Population Genomics in a Disease Targeted Primary Cell Model. Genome Res.
8. Heinzen EL, Ge D, Cronin KD, Maia JM, Shianna KV, et al. (2008) Tissue-specific genetic control of splicing: implications for the study of complex traits. PLoS Biol 6: e1. doi:10.1371/journal.pbio.0060001.
9. Myers AJ, Gibbs JR, Webster JA, Rohrer K, Zhao A, et al. (2007) A survey of genetic human cortical gene expression. Nat Genet 39: 1494–1499.
10. Schadt EE, Molony C, Chudin E, Hao K, Yang X, et al. (2008) Mapping the genetic architecture of gene expression in human liver. PLoS Biol 6: e107. doi:10.1371/journal.pbio.0060107.
11. Lee JH, Park IH, Gao Y, Li JB, Li Z, et al. (2009) A robust approach to identifying tissue-specific gene expression regulatory variants using personalized human induced pluripotent stem cells. PLoS Genet 5: e1000718. doi:10.1371/journal.pgen.1000718.
12. Smirnov DA, Morley M, Shin E, Spielman RS, Cheung VG (2009) Genetic analysis of radiation-induced changes in human gene expression. Nature 459: 587–591.
13. Romanoski CE, Lee S, Kim MJ, Ingram-Drake L, Plaisier CL, et al. Systems genetics analysis of gene-by-environment interactions in human cells. Am J Hum Genet 86: 399–410.
14. Grundberg E, Brandstrom H, Lam KC, Gurd S, Ge B, et al. (2008) Systematic assessment of the human osteoblast transcriptome in resting and induced primary cells. Physiol Genomics 33: 301–311.
15. Chen D, Ji X, Harris MA, Feng JQ, Karsenty G, et al. (1998) Differential roles for bone morphogenetic protein (BMP) receptor type IB and IA in differentiation and specification of mesenchymal precursor cells to osteoblast and adipocyte lineages. J Cell Biol 142: 295–305.
16. Langdahl BL, Kassem M, Moller MK, Eriksen EF (1998) The effects of IGF-I and IGF-II on proliferation and differentiation of human osteoblasts and interactions with growth hormone. Eur J Clin Invest 28: 176–183.
17. Kaji H, Sugimoto T, Kanatani M, Fukase M, Kumegawa M, et al. (1996) Prostaglandin E2 stimulates osteoclast-like cell formation and bone-resorbing activity via osteoblasts: role of cAMP-dependent protein kinase. J Bone Miner Res 11: 62–71.
18. Yao Z, Li P, Zhang Q, Schwarz EM, Keng P, et al. (2006) Tumor necrosis factor-alpha increases circulating osteoclast precursor numbers by promoting their proliferation and differentiation in the bone marrow through up-regulation of c-Fms expression. J Biol Chem 281: 11846–11855.
19. Kim HJ, Zhao H, Kitaura H, Bhattacharyya S, Brewer JA, et al. (2006) Glucocorticoids suppress bone formation via the osteoclast. J Clin Invest 116: 2152–2160.
20. Locklin RM, Khosla S, Turner RT, Riggs BL (2003) Mediators of the biphasic responses of bone to intermittent and continuously administered parathyroid hormone. J Cell Biochem 89: 180–190.
21. Panda DK, Miao D, Bolivar I, Li J, Huo R, et al. (2004) Inactivation of the 25-hydroxyvitamin D 1alpha-hydroxylase and vitamin D receptor demonstrates independent and interdependent effects of calcium and vitamin D on skeletal and mineral homeostasis. J Biol Chem 279: 16754–16766.
22. Pastinen T, Ge B, Gurd S, Gaudin T, Dore C, et al. (2005) Mapping common regulatory variants to human haplotypes. Hum Mol Genet 14: 3963–3971.
23. Verlaan DJ, Ge B, Grundberg E, Hoberman R, Lam KC, et al. (2009) Targeted screening of cis-regulatory variation in human haplotypes. Genome Res 19: 118–127.
24. Ge B, Gurd S, Gaudin T, Dore C, Lepage P, et al. (2005) Survey of allelic expression using EST mining. Genome Res 15: 1584–1591.
25. Pastinen T, Sladek R, Gurd S, Sammak A, Ge B, et al. (2004) A survey of genetic and epigenetic variation affecting human gene expression. Physiol Genomics 16: 184–193.
26. Ge B, Pokholok DK, Kwan T, Grundberg E, Morcos L, et al. (2009) Global patterns of cis variation in human cells revealed by high-density allelic expression analysis. Nat Genet 41: 1216–1222.
27. Laitinen A, Altraja A, Kampe M, Linden M, Virtanen I, et al. (1997) Tenascin is increased in airway basement membrane of asthmatics and decreased by an inhaled steroid. Am J Respir Crit Care Med 156: 951–958.
28. Idaghdour Y, Czika W, Shianna KV, Lee SH, Visscher PM, et al. (2010) Geographical genomics of human leukocyte gene expression variation in southern Morocco. Nat Genet 42: 62–67.
29. Smith EN, Kruglyak L (2008) Gene-environment interaction in yeast gene expression. PLoS Biol 6: e83. doi:10.1371/journal.pbio.0060083.

30. Cunninghame Graham DS, Graham RR, Manku H, Wong AK, Whittaker JC, et al. (2008) Polymorphism at the TNF superfamily gene TNFSF4 confers susceptibility to systemic lupus erythematosus. Nat Genet 40: 83–89.
31. Deblois G, Giguere V (2008) Nuclear receptor location analyses in mammalian genomes: from gene regulation to regulatory networks. Mol Endocrinol 22: 1999–2011.
32. Reddy TE, Pauli F, Sprouse RO, Neff NF, Newberry KM, et al. (2009) Genomic determination of the glucocorticoid response reveals unexpected mechanisms of gene regulation. Genome Res 19: 2163–2171.
33. Midwood K, Sacre S, Piccinini AM, Inglis J, Trebaul A, et al. (2009) Tenascin-C is an endogenous activator of Toll-like receptor 4 that is essential for maintaining inflammation in arthritic joint disease. Nat Med 15: 774–780.
34. Zhao Y (1999) Tenascin is expressed in the mesenchyme of the embryonic lung and down-regulated by dexamethasone in early organogenesis. Biochem Biophys Res Commun 263: 597–602.
35. Wang D, Chen H, Momary KM, Cavallari LH, Johnson JA, et al. (2008) Regulatory polymorphism in vitamin K epoxide reductase complex subunit 1 (VKORC1) affects gene expression and warfarin dose requirement. Blood 112: 1013–1021.
36. Gentleman RC, Carey VJ, Bates DM, Bolstad B, Dettling M, et al. (2004) Bioconductor: open software development for computational biology and bioinformatics. Genome Biol 5: R80.
37. Bolstad BM, Irizarry RA, Astrand M, Speed TP (2003) A comparison of normalization methods for high density oligonucleotide array data based on variance and bias. Bioinformatics 19: 185–193.
38. Irizarry RA, Hobbs B, Collin F, Beazer-Barclay YD, Antonellis KJ, et al. (2003) Exploration, normalization, and summaries of high density oligonucleotide array probe level data. Biostatistics 4: 249–264.
39. Baldi P, Long AD (2001) A Bayesian framework for the analysis of microarray expression data: regularized t -test and statistical inferences of gene changes. Bioinformatics 17: 509–519.
40. Storey JD, Tibshirani R (2003) Statistical significance for genomewide studies. Proc Natl Acad Sci U S A 100: 9440–9445.
41. Purcell S, Neale B, Todd-Brown K, Thomas L, Ferreira MA, et al. (2007) PLINK: a tool set for whole-genome association and population-based linkage analyses. Am J Hum Genet 81: 559–575.
42. Li Y, Abecasis G (2006) Mach 1.0: Rapid Haplotype Reconstruction and Missing Genotype Inference. Am J Hum Genet S79 2290.
43. Li Y, Willer C, Sanna S, Abecasis G (2009) Genotype imputation. Annu Rev Genomics Hum Genet 10: 387–406.
44. Li Y, Willer C, Ding J, Scheet P, Abecasis G (2006) Rapid Markov Chain Haplotyping and Genotype Inference. Submitted.
45. Hao K, Chudin E, McElwee J, Schadt EE (2009) Accuracy of genome-wide imputation of untyped markers and impacts on statistical power for association studies. BMC Genet 10: 27.
46. Browning SR, Browning BL (2007) Rapid and accurate haplotype phasing and missing-data inference for whole-genome association studies by use of localized haplotype clustering. Am J Hum Genet 81: 1084–1097.
47. (2000) Long-term effects of budesonide or nedocromil in children with asthma. The Childhood Asthma Management Program Research Group. N Engl J Med 343: 1054–1063.
48. Himes BE, Hunninghake GM, Baurley JW, Rafaels NM, Sleiman P, et al. (2009) Genome-wide association analysis identifies PDE4D as an asthma-susceptibility gene. Am J Hum Genet 84: 581–593.
49. Tantisira KG, Lake S, Silverman ES, Palmer LJ, Lazarus R, et al. (2004) Corticosteroid pharmacogenetics: association of sequence variants in CRHR1 with improved lung function in asthmatics treated with inhaled corticosteroids. Hum Mol Genet 13: 1353–1359.